JOURNAL OF CATALYSIS 96, 222–233 (1985)

Mechanism for Propylene Oxidation to Acrolein on $Bi_2Mo_3O_{12}$: A Quantum Chemical Study

ALFRED B. ANDERSON,* DAVID W. EWING,* YUNSOO KIM,* ROBERT K. GRASSELLI,† JAMES D. BURRINGTON,† AND JAMES F. BRAZDIL†

Chemistry Department, Case Western Reserve University, Cleveland, Ohio 44106; and †Department of Research and Development, The Standard Oil Company (Ohio), 4440 Warrensville Center Road, Warrensville Heights, Ohio 44128

Received February 14, 1985; revised June 8, 1985

The selective oxidation of propylene to acrolein on α-bismuth molybdate has been studied using molecular orbital theory and a surface cluster model. The overall reaction is $H_2C{=}CHCH_3 + O_2 \rightarrow H_2C{=}CHCHO + H_2O$. We find propylene can first coordinate to surface Mo^{VI} through a π-donation bond, and α-hydrogen abstraction proceeds to a bismuth oxygen anion with a low barrier yielding an allyl–Mo^{V} complex. The transition state involves a $CH{-}O^{2-}$ σ-donation stabilization and the activation is a result of the filled $CH{-}O^{2-}$ σ* antibonding counterpart orbital being stabilized though mixing with the π* orbital on the olefinic end. Allyl then forms a σ bond to a neighboring surface oxygen atom bonded to molybdenum, and the catalytic site is reduced by a second electron. It is postulated that these electrons may flow through the Mo 4*d* conduction band to a remote site active for O_2 reduction. The σ-allyl rotates easily so that either end carbon may receive oxygen. The second dehydrogenation step is accompanied by a second two-electron reduction of the surface. It is postulated that this step may be activated by the concomitant reoxidation of the bismuth site as water desorbs. After acrolein desorption, the oxygen vacancy is postulated to migrate to the site of earlier oxygen reduction.

INTRODUCTION

Mechanistic features of selective oxidations of olefins using bismuth molybdate catalysts have been reviewed recently (*1*). The purpose of this paper is to present a quantum chemical study of propylene ($H_2C{=}CHCH_3$) oxidation to acrolein ($H_2C{=}CHCH{=}O$) over α-bismuth molybdate, $Bi_2Mo_3O_{12}$, and use the results to interpret experiment. Though, as will be seen, much of the experimental evidence is circumstantial, based on clever detective work, general features of the oxidation mechanism are generally accepted which are believed to hold for α-bismuth molybdate and the β-($Bi_2M_2O_9$) and γ-(Bi_2MoO_6) forms as well. The first step is α-hydrogen abstraction from propylene, which is the rate-determining step with a barrier of 19–21 kcal/mole (*2*, *3*), to form an allylic species on the surface of the catalyst (*4*, *5*). The abstracted hydrogen is thought to bond to an oxygen anion bonded to bismuth (*6*, *7*) because α-hydrogen abstraction is seen on Bi_2O_3, where the allylic species combine to form 1,5-hexadiene, with no further oxidation to acrolein or other oxidation products. MoO_3 is relatively inactive toward propylene; however, *in situ* generation of allyl radicals over MoO_3 does produce acrolein and other oxidation products (*7*); this is taken as evidence that oxygen bonded to molybdenum will not abstract α-hydrogen but will insert into the adsorbed allylic species during acrolein formation over bismuth molybdates. The formation of higher oxidation products than acrolein over MoO_3 may be related to the facility of MoO_3 to disporportionate to MoO_2 and O_2 (*8*). While bismuth molybdates can also disproportionate on heating (*9*), $^{18}O_2$ exchange experiments show a higher oxygen binding energy for bismuth molybdates than for MoO_3: the ex-

0021-9517/85 $3.00

change barrier is 67 kcal/mole for $Bi_2Mo_3O_{12}$ and 56 kcal/mole for MoO_3 (*10*). On Bi_2O_3 the $^{18}O_2$ exchange barrier is even lower, 38 kcal/mole (*10*), yet oxygen does not insert into allyl on this oxide, probably because dimerization is a more favorable reaction in the absence of the π-donation coordination center which is available with Mo^{VI} centers in the other oxides. As we have shown in a recent theoretical study, there are no low-lying empty levels for allylic π-donation bonding on α-, β-, and δ-Bi_2O_3 (*11*). In fact, the Bi orbitals nearest in energy to π orbitals in allyl are completely filled and have considerable O $2p$ mixing, so that a closed-shell interaction between allyl and the Bi^{III} centers is expected to prevent strong allyl coordination to Bi^{III}. The weak bonding of allyl to Bi_2O_3 allows dimerization while on MoO_3 the π-donation bond to Mo^{VI} presumably sets the stage for oxygen insertion.

The reaction so far can be written

$$H_2C{=}CH\underset{H}{C}{:}H + :\ddot{O}:^{2-} \rightarrow$$

$$H_2C{\cdots}CH{\cdots}CH_2 + H{:}\ddot{O}{:}^{1-} + e^- \quad (1)$$

The electron is expected to reduce Mo^{VI} to Mo^{V} with allyl complexing with it:

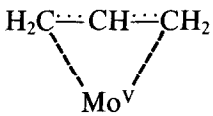

Substituent effect studies exclude the formation of an allyl anion (*12*) or an allyl cation + Mo^{IV} (*13*, *14*) as alternatives.

The next step is believed to be the formation of an allylic intermediate σ-bonded to oxygen in the surface of the catalyst. Evidence for this is seen in ultraviolet photoemission (UPS) (*9*) and IR vibrational studies (*15*). Recent work (*16*a) shows, in the case of α-bismuth molybdate, that the σ complex is with oxygen which is bonded to molybdenum. When propylene is absorbed, there is an immediate shift in the MoO frequency corresponding to the formation of a hydrocarbon intermediate bonded to MoO. When the catalyst is reduced with butene, which dimerizes, there is no shift in the MoO frequency. Oxygen isotope studies (*16*b) agree: when the catalyst is prereduced with butene and reoxidized with ^{18}O and then reacted with propylene, no ^{18}O appears in the acrolein product. However, when propylene is used for the reduction, followed by ^{18}O reoxidation, ^{18}O appears in the acrolein product when propylene is oxidized. These studies show there are two types of oxygen in the surface of the catalyst. Oxygen bonded to molybdenum inserts in the allylic intermediate and some other oxygen, presumably bonded to bismuth, abstracts hydrogen from propylene.

The adsorbed allylic species takes two forms, as shown by the reaction of [1,1-$^2H_2$]allyl alcohol which yields both [1-$^2H_1$] and [3,3-$^2H_2$]acrolein (*17*). It is believed that the allylic intermediate is π-coordinated to Mo^{VI} centers either symmetrically or in a readily reversible $C_1C_2 \rightleftarrows C_2C_3$ π complex. An equilibrium between two intermediates σ-bonded to oxygen of the form $C_1O \rightleftarrows C_3O$ or possibly a di-σ-bonded allyl is also consistent with the data of Ref. (*17*). The formation of a σ intermediate from propylene may be written

$$OH^{1-} + Mo^{V}\,C_3H_5 + Mo^{VI} + :\ddot{O}:^{2-} \rightarrow$$

$$OH^{1-} + Mo^{IV} + Mo^{V} + H_2C{=}CH\underset{H}{C}{:}\ddot{O}{:} \quad (2)$$

and since molybdenum is reduced, there may be an activation barrier. In bulk MoO_3, the gap from the filled oxygen anion $2p$ band to the bottom of the Mo^{V} $4d$ conduction band is ~3 eV (*11*), but the barrier will be less than $3 \times 3 = 9$ eV because the CO bond forms and because Mo $4d$ surface states will lie somewhere in the band gap due to the partial coordination of surface molybdenum cations (the Mo $4d$ band is antibonding to the O $2p$ band). Furthermore, in an oxidizing environment, these

electrons may be stabilized by reducing O_2 at the catalyst surface, by reducing cation vacancies, or by structural rearrangements. Thus, it is expected that the $C_1C_2 \rightleftarrows C_2C_3$ or symmetric σ-allylic intermediate is responsible for the formation of both [1-$^2H_1$] and [3,3-$^2H_2$]acrolein products. This point will be addressed in our theoretical study below.

The existence of an isotope effect for allylic hydrogen abstraction from [1,1-$^2H_2$]allyl alcohol (k_H/k_D = 2.5) has been taken to imply the hydrogen abstraction is the rate-determining step in acrolein formation from allyl alcohol (*17*). The final step in acrolein formation is written

$$\begin{aligned} OH^{1-} + Mo^{IV} + Mo^{V} \\ + H_2C{=}CHC{:}\ddot{O}{:} \rightarrow H_2O + Mo^{IV} \\ + Mo^{IV} + H_2C{=}CHCHO \end{aligned} \quad (3)$$

The aldehydic hydrogen abstraction barrier is expected to be lower than that for the initial α-hydrogen abstraction from propylene because of the known weakness of aldehydic CH bonds. Vibrational spectroscopy in the local mode model (unrelaxed hydrocarbon framework during the CH stretch) yields an aldehydic CH bond strength of 87 kcal/mole (*18*) and a propylene α-hydrogen CH bond strength of 104 kcal/mole for in-plane bonds and 111 kcal/mole for out-of-plane bonds (*19*).

The final steps in the overall reaction in the formal scheme being outlined are the desorption of acrolein and water, leaving behind two oxygen vacancies, each of charge −2. If not already oxidized during the earlier steps, the electrons in these vacancies are expected to be in stabilized molybdenum 4*d* band orbitals lying in the O 2*p*–Mo 4*d* band gap. One of the vacancies, the one created when oxygen bonded to molybdenum inserts in allyl, is believed to migrate some distance through the bulk of the catalyst, experiencing activation barriers to migration. The other anion vacancy, believed to be coordinated to bismuth, remains at the surface and is rapidly oxidized by O_2; activation energies are 1.3, 8.1, and 1.2 kcal/mole for α-, β-, and γ-bismuth molybdate, respectively (*20*). Activation barriers to reoxidizing the bulk vacancies are around 25–27 kcal/mole for α- and β-bismuth molybdate and ~8 kcal/mole for the γ form (*20*). The low barrier for the γ form is apparently a result of the presence of layers of MoO_3 octahedra in this phase. These octahedra are more dispersed in the other phases. Restructuring of the MoO_3 octahedra within the layers in the γ phase is thought to accompany the vacancies, stabilizing the transition states which they pass through during migration (*20*). Anion vacancy migration activation energies have been estimated to be 20–23 kcal/mole in MoO_3 (*21, 22*), suggesting the γ form of bismuth molybdate has particularly favorable structural or electronic properties for rapid anion vacancy migration.

THEORY

Electronic Properties of α- and γ-Bismuth Molybdate

In our recent theoretical study (*11*) of MoO_3 and α, β, and δ phases of Bi_2O_3, we established the salient features of the electronic structures of these oxides. In MoO_3 the oxygen anion band was completely filled and the Mo^{VI} conduction band was empty. The band gap, based on an $Mo_6O_{24}^{14-}$ cluster, was 3.6 eV, a little larger than experimental estimates of 2.8 (*23*)–3.2 eV (*24, 25*). The various phases of Bi_2O_3 had four filled bands: the lowest was O 2*p* with a small Bi 6*s* bonding component, the next was Bi 6*s* with a large O 2*p* bonding and small O 2*s* antibonding component, the next was O 2*p* with a large Bi 6*p* bonding component, and the top one was Bi 6*s* and 6*p* with a large O 2*p* antibonding component. The top three bands agreed qualitatively with ultraviolet photoemission studies (*26*). It may be expected that because

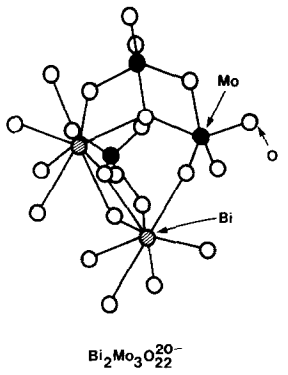

FIG. 1. α-Bismuth molybdate cluster model used to obtain the predicted electronic structure of Fig. 2.

Mo^{VI} and Bi^{III} are approximately octahedrally coordinated to oxygen anions in the various bismuth molybdates, the electronic structures of the mixed metal oxides would, to a good approximation, be given as a superposition of the components. This is found to be the case for a $Bi_2Mo_3O_{22}$ cluster model of α-bismuth molybdate shown in Fig. 1. This cluster represents a small piece of the unit cell of $Bi_2Mo_3O_{12}$, for which structure parameters are available (*27*). The correlation diagram showing the electronic structure (Fig. 2) was determined using the cation parameters of Ref. (*11*) for MoO_3 and Bi_2O_3 and averaging the corresponding anion parameters within the ASED-MO

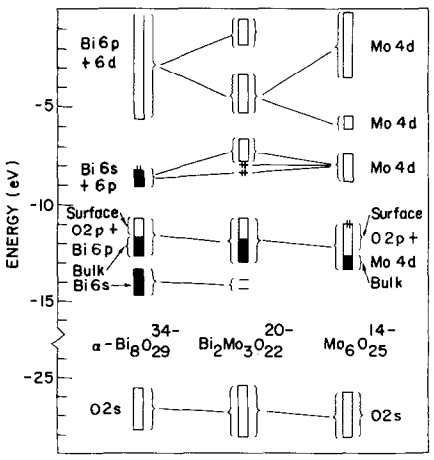

FIG. 2. Correlation of electronic structures of α-Bi_2O_3 and MoO_3 with α-bismuth molybdate.

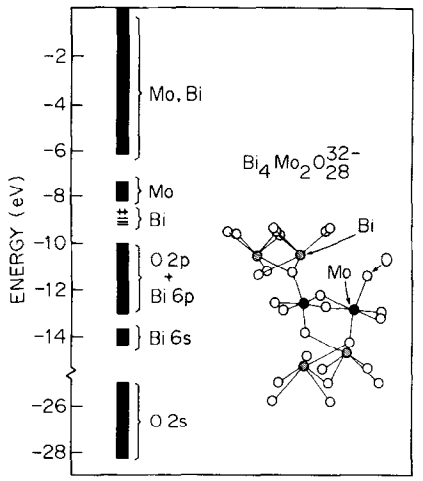

FIG. 3. Cluster model and calculated electronic structure for γ-bismuth molybdate.

procedure used in Ref. (*11*) and the present work. It may be seen that the O 2*p* band is indeed an average of the O 2*p* bands in MoO_3 and α-Bi_2O_3 (electronic structures of the various phases of Bi_2O_3 are similar (*11*)). The Bi 6*s* + 6*p* band lies at the bottom of the Mo 4*d* band. Unfortunately, there are no published photoemission or optical studies for comparison. It would appear that $Bi_2Mo_3O_{12}$ is a low band gap semiconductor. A similar calculation has been made using a $Bi_4Mo_2O_{28}^{32-}$ cluster fragment of the layered Bi_2MoO_6 γ structure (*28*) shown in Fig. 3. This yields a similar electronic structure. A photoemission spectrum of this phase has been published (*9*), and is similar to MoO_3, i.e., there is no evident emission from the Bi 6*p* + 6*s* band. This sample was oxidized at 470°C for 1 h under 1 atm of oxygen. Might this treatment have segregated MoO_3 at the surface, so that the spectrum is that of MoO_3? Or, might have the excess oxygen oxidized the Bi 6*p* + 6*s* band electrons, creating O^{2-} or O^{1-} on the surface? The O 1*s* emission spectrum of an initial sample outgassed at 120°C shows a shoulder corresponding to O^{1-}, which disappears on outgassing at a higher temperature. Would this sample show emission from the Bi 6*s* + 6*p* band? Emission from Bi 4*f* and

TABLE 1

Atomic Parameters Used in the Calculations[a]

Atom	Orbital	Slater exponent (a.u.)	Ionization potential (eV)
Bi	6*s*	2.35	14.5
	6*p*	2.35	9.79
	6*d*	2.05	4.35
Mo	4*d*	4.542 (0.5899)[b] 1.901 (0.5899)[b]	10.06
	5*s*	2.256	9.1
	5*p*	1.956	5.92
O	2*s*	1.896	26.23
	2*p*	1.877	11.37
C	2*s*	1.658	18
	2*p*	1.618	9.26
H	1*s*	1.2	11.6

[a] See Ref. (*11*) and the text.
[b] Double-zeta *d*; linear parameters in parentheses.

Mo 3*d* levels indicate both are present at the surface of this sample. Experimental work on these questions would be worthwhile.

Adsorption of Propylene to α-Bismuth Molybdate

The $Bi_2Mo_3O_{20}^{12-}$ cluster model chosen for the catalysis mechanism study has all the cations nearly in a plane and is bulk superimposable. The Mo^{VI} site chosen for propylene coordination is coordinatively unsaturated. Such sites are expected to exist and to be π acceptor sites. Support for the belief such sites exist lies in recent studies of methanol oxidation which show the (010) surface is inactive (*29*); this is the surface created easily by crystal cleavage and is covered by anions. Cleavage perpendicular to these planes necessarily creates unsaturated Mo^{VI} centers to which methanol coordinates. Subsequent steps lead to the formation of formaldehyde, water, and reduced molybdenum oxide (*29*). Thus we assume such sites for our model. The bismuth cations are fully coordinated in the model and one of them has an O^{2-} anion in a position where it can accept an α-hydrogen atom from propylene. The cation band is assumed to be empty at the surface in the oxidizing environment. Several O^{2-} anions which bridge the active Mo^{VI} center with nearby Mo^{VI} and Bi^{III} cations are present nearly in the cation plane to participate in the oxygen insertion step. In our model work structure relaxations of the atoms making up the surface cluster are not considered. Theory parameters are in Table 1.

Propylene π coordinates with a calculated stability of 26 kcal/mole with a structure as shown in Fig. 4. The carbon double bond stretches 0.04 Å from the calculated gas-phase value, the single-bond length does not change, and the olefinic hydrogen atoms and the methyl group bend several degrees away from the surface. The bonding is predominantly π donation as shown in Fig. 5. It is also evident in Fig. 5 that the model of a fully oxidized surface cation band is being used and that two Mo 4*d* levels have been stabilized on the active Mo^{VI} cation due to the incomplete coordination (compare with Fig. 2). There is no significant Mo 4*d* backbonding into the propylene π^* orbital because the *d* band is empty.

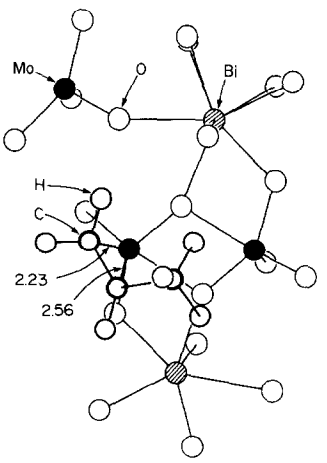

FIG. 4. Propylene adsorption on a cluster model of an α-bismuth molybdate surface.

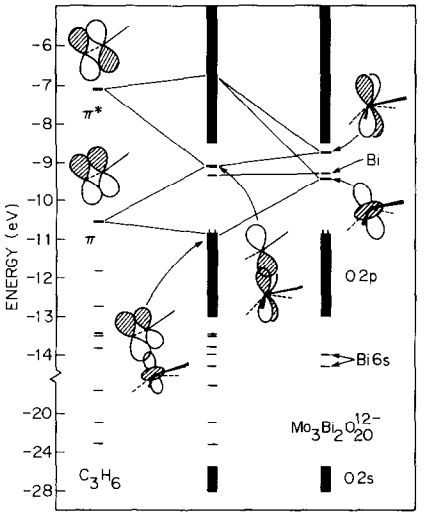

FIG. 5. Bonding interactions between adsorbed propylene and a surface Mo^{VI} cation (See Fig. 4).

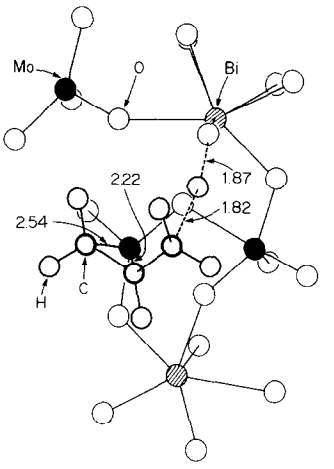

FIG. 6. Transition state for α-hydrogen abstraction from propylene.

Abstraction of α-Hydrogen from Propylene

At the temperatures of active catalysis, 300–450°C (*1*), adsorbed propylene will be in dynamic equilibrium with the gas phase because the positive $-T\,\Delta S$ contribution to the free energy of adsorption can overcome our 26 kcal/mole approximation to the negative adsorption enthalpy. However, propylene should linger adsorbed long enough at active Mo^{VI} sites for α-hydrogen abstraction to take place. To study this step, adsorbed propylene is rotated until an out-of-plane methyl CH bond is directed toward an oxygen anion coordinated to bismuth and then this bond is stretched 0.62 Å to a transition state where it is 1.3 Å from the oxygen anion. The structure at the transition state is in Fig. 6. The hydrocarbon framework stucture is optimized with the double bond stretching 0.02 Å and the CC single bond contracting 0.12 Å from those for adsorbed propylene. The calculated activation energy is 25 kcal/mole, a bit greater than the 19–21 kcal/mole experimental range (*21*). This overestimate may stem from the approximations of the ASED-MO theory, the surface model chosen, and from the omission of surface structured relaxations in this model study. The CH bond is activated by forming a stabilizing three-center CH–O σ-donation bond with the O^{2-} cation bonded to bismuth as shown in Fig. 7. The stabilization is made clear by the comparison of the σ level in uncoordinated transition-state structure propylene with its position in the transition-state complex. This type of CH activation has been found in theoretical studies using the ASED-MO theory for α-hydrogen abstraction from propylene chemisorbed to Pt(111) (*30*), and for ethylenic (*30*) and acetylenic (*31*) CH bonds, and for OH (*32*) and HCl (*33*) bonds as well. The CH–O antibonding counterpart orbital is occupied and appears in the

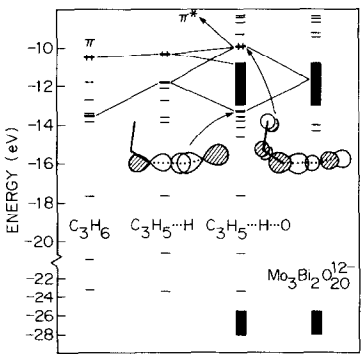

FIG. 7. The σ-donation bond between the transition state CH bond and surface oxygen as in Fig. 6.

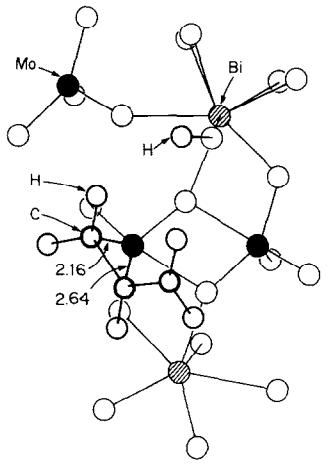

FIG. 8. Structure of π-allyl plus adsorbed OH.

O 2*p*-cation band gap, as shown in Fig. 7. *This orbital is stabilized by hybridization with propylene π and π^* orbitals.* The products, π-coordinated allyl and OH^-, have a calculated stability of 19 kcal/mole with respect to gas-phase propylene; the CC double and single bonds are 0.02 and 0.08 Å shorter than in adsorbed propylene; the structure may be seen in Fig. 8. Figure 9 illustrates how the highest occupied level in the π-allyl complex is a hybridized mixture of the three allylic π orbitals donating into a molybdenum *d* orbital. The carbon charge in π-complexed propylene was +0.5 and the molybdenum charge was 1.9. Now these charges are −0.1 and 1.65; thus 0.85 electron has been transferred to the Mo–allyl complex, which accounts for 0.85 electron lost by the O^{2-} anion which has become a OH^- anion. This means allyl should behave like a neutral species, which has been deduced from substituent effect studies (*12–14*), as discussed in the Introduction. However, the Mo–allyl π complex is formally reduced by one electronic charge, marking the first step toward catalyst reduction.

Formation of an Allyl Intermediate σ-Bonded to Oxygen

Thermodynamics does not favor a long-lived π-allylic intermediate, unless there is a hydrogen sink, such as water formation, because of the high reaction temperature and the low stability of the intermediate with respect to gas-phase propylene. The next step of the process requires allyl to either lose the second hydrogen or bond to surface oxygen. It is more reasonable to explore the latter course because of the weakness of the subsequent aldehydic CH bonds (*18*) and the experimental conformation of surface σ-bonded allylic species (*9, 15, 16*).

The formation of the σ-allyl–oxygen intermediate appears to require the promotion of two electrons up to the cation conduction band, leading to instability. This is because the antibonding counterpart to the C–O σ bond is doubly occupied (Fig. 9). We expect these electrons make their way to an active site and dissociatively reduce O_2. As soon as electrons arrive at such a site, a reaction of the form

$$\tfrac{1}{2}O_2 + MoO_2 \rightarrow MoO_3$$

can take place with an enthalpy of −50 kcal/mole (*34*). This is a strong driving force. At a later step, when acrolein has desorbed, an uncharged anion vacancy will diffuse to the O_2 adsorption site and the surface vacancy will be filled. As an alternative, reduction of the surface may be promoted by structural relaxations, which can stabilize Mo 4*d* states to positions as low as

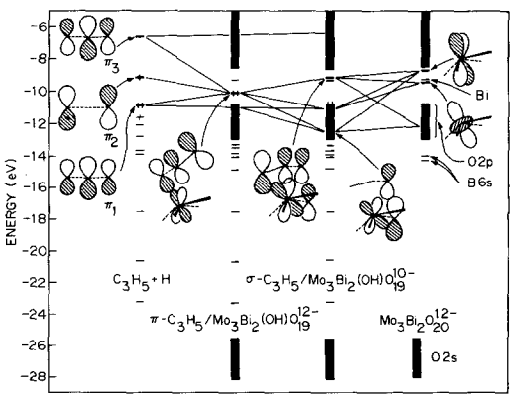

FIG. 9. Correlation between π-bonding in π-allyl and π- and σ-bonding in σ-allyl.

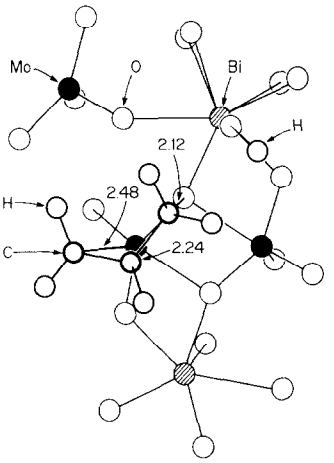

FIG. 10. Structure of σ-allyl plus adsorbed OH.

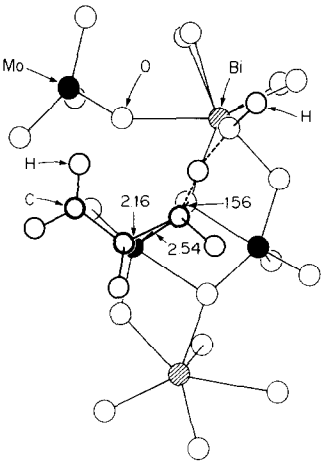

FIG. 12. Transition state for dehydrogenation of σ-allyl.

0.9 eV above the top of the O 2*p* valence band (*8*). We have not explored such relaxations, but the occurrence of stabilized Mo^V or Mo^{IV} may allow surface reoxidation to occur at a later stage after desorption of the acrolein product. We do not know precisely the position of the bottom of the conduction band relative to the occupied allylic π^* orbital and therefore do not know the activation energy for σ-allyl formation. However, this is known to not be the rate-limiting step and the barrier is less than that for α-hydrogen abstraction, as no π-allyl has been characterized on bismuth molybdates. From Fig. 9 it is evident that π-bonding to molybdenum persists in the σ intermediate. O_2 reduction is not being modeled in the calculations either, but it should stabilize the system by about 50 kcal/mole. We model the stability increase crudely by assuming the electrons reduce O_2 at a remote site and remove them from the cluster model. This produces a stability of 50 kcal/mole for σ-allyl; the structure is shown in Fig. 10. This stability gain should probably be viewed as an upper limit; in the case that the surface is not immediately reoxidized, the gain is likely to be less.

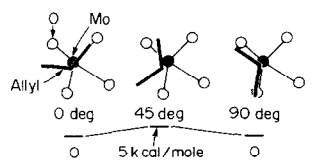

FIG. 11. Barrier to rotating σ-allyl.

A 5 kcal/mole barrier is calculated for rotating allyl 90 degrees so that σ bonds form between both end carbon atoms and surface oxygens, as shown in Fig. 11. This conformation has identical stability. Thus, either end can lose a hydrogen atom, as shown by the labeling studies (*17*) discussed in the Introduction.

Loss of Aldehydic Hydrogen and Acrolein Formation

In the model chosen for aldehydic dehydrogenation, allyl is rotated so that the CH bond is directed approximately toward the OH group, which is bent away as in Fig. 12. This gives rise to CH donation to the oxygen of the hydroxyl group, and the antibonding counterpart begins to move up into the O 2*p*-conduction band gap, bearing two electrons. These electrons will reduce the surface. A high barrier of ~40 kcal/mole is calculated for this process, suggesting oxidation of the surface or the formation of stable reduction sites must accompany aldehydic dehydrogenation. It may be noted that transferring the hydrogen to an oxygen

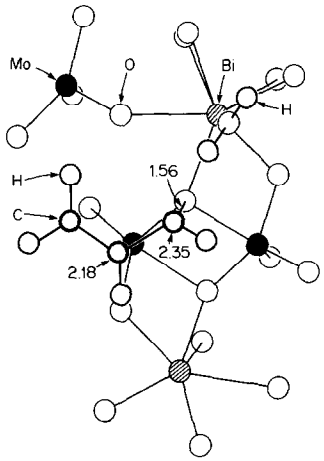

FIG. 13. Adsorbed acrolein and water products (see text).

anion instead of hydroxyl would have similar energetics. When these electrons are removed at the start of the reaction, the barrier is reduced to ~15 kcal/mole. The products, absorbed acrolein and water, are shown in Fig. 13. Since, as discussed in the Introduction, the reoxidation step involves oxygen vacancies on bismuth, and since no thermodynamic data has been found for bismuth oxide in lower oxidation states, the reoxidation energy is less certain than it is for molybdenum oxide. However, the assumption that it is 50 kcal/mole as for Eq. (4) is employed. The water desorption energy is calculated to be 30 kcal/mole, and so a combination of entropy and the possible displacement by oxygen of the water molecule as it forms should cause it to desorb rapidly, with a net stabilization of 20 kcal/mole.

In our model, the calculated energy for acrolein desorption is 46 kcal/mole. This number appears high, but omits stabilizing relaxations around the oxygen vacancy. The overall estimated heat of the catalytic formation of acrolein and water:

$$C_3H_6 + O_2 \rightarrow C_3H_4O + H_2O \qquad (5)$$

is then 44 kcal/mole. The experimental value is about 72 kcal/mole, based on standard thermal chemical data (*34*). The ~28-kcal/mole error is not bad for theory considering that two 99 kcal/mole C—H bonds and one 116 kcal/mole O=O bond were broken and two 111 kcal/mole O—H and 174 kcal/mole C=O bonds were formed. The energetics for the overall process are given in Fig. 14.

DISCUSSION

Not much is known about the structure and composition of α-bismuth molybdate during the catalytic oxidation of propylene to acrolein. In this theoretical study we have modeled a fully oxidized surface which should represent the most active situation, and which should exist in the presence of oxygen. We have postulated that some bismuth centers are coordinatively saturated with oxygen anions when at the surface and that some molybdenum cations at the surface may have unsaturated sites as found on certain faces of MoO_3 crystals. The actual surface structure or structures are unknown, but a cluster model which is bulk superimposable and possesses an unsaturated molybdenum site, surface oxygen bonded to molybdenum and surface oxygen bonded to bismuth has been chosen. The energies we calculate for various steps of the oxidation might be somewhat changed

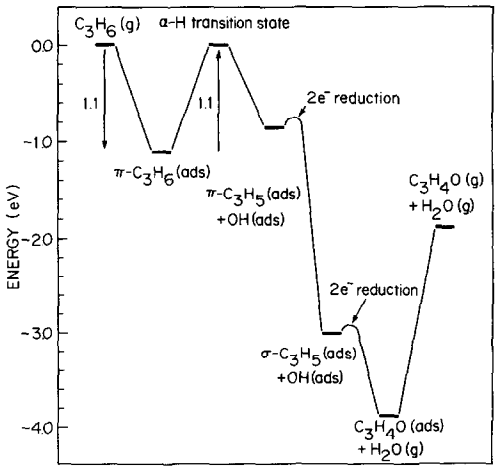

FIG. 14. Energetics calculated for the reaction steps according to postulates concerning the reduction steps as discussed in the text.

by cluster relaxations which were not tried because of the prohibitively large number of variables involved, but, by the same token, the choice of a different surface cluster model might also have influenced the calculated energetics. Furthermore, the approximate nature of the ASED-MO theory renders all results numerically approximate. For these reasons, the proper emphasis is on the qualitative aspects of the steps of the oxidation.

We have found that the α-hydrogen abstraction is activated on the surface and that the coordination of allyl to the molybdenum center is probably what keeps allyl from dimerizing or even from desorbing as seen recently for the Bi_2O_3 surface (*35*). The allylic species has the characteristics of an allyl radical covalently bonded to a Mo^V center. The next postulated step of π-allyl formation requires the promotion of two electrons to the cation band. This is relatively easy to do because of the stability of Mo^{IV} centers, but would be very difficult to accomplish on a stoichiometric Bi_2O_3 surface because the bottom of the bismuth 6*p* band lies much higher in energy. Furthermore, structural rearrangements (corner to edge-shared MoO_6 pseudooctahedra) are known to occur with the Mo^{VI} to Mo^{IV} oxide transformation; these stabilize the reduction, but no such transformations are known for the bismuth oxides. The formation of allyl radicals and their dimerization on Bi_2O_3 requires the reduction of the surface by one electron per radical formed. The fact that this occurs suggests that the surface may be nonstoichiometric and rich in oxygen with some holes in the highest occupied Bi 6*s* + 6*p* band. These holes are then reduced as the allyl radicals form but further oxidation is probably prevented since the hole population will be depleted, thereby preventing oxygen insertion, a step requiring further reduction of the surface.

We have modeled the cation band as completely empty in our cluster model of α-bismuth molybdate, though in fact it may be that the bismuth 6*s* + 6*p* levels are at least partially occupied, so that bismuth is nearly in the +3 oxidation state. A self-consistent quantum mechanical approach might shift these energy levels to a position below the empty Mo^{VI} 4*d* band if this is the actual state of surface bismuth. We could have modeled this oxidation state by constraining the orbital occupations so that electrons remain in the bismuth levels but this would not have changed our results because these orbitals do not participate in bonding to the intermediates during the catalysis. For the sake of convenience, then, we have treated bismuth as Bi^V, though the results should be the same for Bi^{III}. If Bi^V actually does exist on the suface due to excess surface oxygen, then the empty Bi 6*s* + 6*p* band must correlate with the filled band in the bulk.

Once the two-electron reduction takes place and allyl is σ-bonded to surface oxygen, the intermediate enjoys considerable covalent bonding to the adjacent molybdenum center. This is likely to be why it is an oxygen anion bonded to molybdenum which inserts in the acrolein product. Furthermore, the σ bonding that allyl experiences following the abstraction of an α-hydrogen may prevent the movement of allyl to some site where a bismuth oxygen might insert instead. After σ-allyl forms, it is easy to rotate it around so that oxygen can insert on either end carbon atom in the product.

We have coupled the first two-electron reduction with O_2 reduction at a remote active molybdenum site. This requires electron flow through the molybdenum 4*d* band. Such a process seems more likely than structural rearrangements stabilizing reduced molybdenum centers because, as yet, no oxygen vacancy has been formed; this requires acrolein desorption. However, structural relaxations leading to stabilization cannot be ruled out.

The second (aldehydic) hydrogen-loss step is accompanied by a second two-electron reduction of the surface. To keep the barrier for this process low, it has been necessary to assume that concomitant reoxida-

tion is occurring. It is possible that this step is activated by some other mechanism, but no such mechanism is evident at present. In the α-hydrogen abstraction case, the π-allyl + Mo *d* complex is able to absorb the two CH–O antibonding electrons and activate the process using the low-lying complex orbital. Of course, it may be that the π-allyl intermediate forms so rapidly that π-allyl never exists for a significant length of time. However, the agreement between the calculated and experimental α-hydrogen activation energies suggests it does form, and the reduction accompanying σ-allyl formation occurs subsequently; otherwise the α-hydrogen abstraction barrier might be smaller. For aldehydic hydrogen activation no mechanism appears to be available for removing the two CH–O antibonding electrons other than concomitant surface reoxidation. The stabilization energy for the bismuth site reoxidation step has been roughly estimated to be the same as for molybdenum dioxide reoxidation, and when coupled with water desorption, the most stable product of the reaction sequence is formed, absorbed acrolein. When acrolein desorbs, structural relaxations and the oxygen vacancy migration process are set in motion, but, as in the earlier steps of our treatment, they are not treated.

CONCLUSIONS

This molecule orbital study has provided detailed information for the α-bismuth molybdate catalyzed selective oxidation reaction which yields acrolein from propylene. The CH activation and two-electron reduction steps have been found explicable in terms of molecular orbital bonding theory and the electronic structure of the solid catalyst. An uncertainty about the oxidation state of the bismuth has been found and this question would be interesting to pursue experimentally and with self-consistent quantum chemical calculations. Because of the large number of structural variables and the lack of knowledge of catalyst surface structure and composition, it has been necessary to postulate structural details. Unless the catalyst surface properties are someday very well determined by experiment, it is doubtful that theory can go beyond the type of surface structure assumptions we have found necessary. However, the bulk structures of bismuth molydate catalysts are known, and so the catalyst reoxidation step by means of oxygen vacancy diffusion may be a worthwhile topic for quantum chemical studies.

ACKNOWLEDGMENTS

We thank Teresa Gordon for assistance with some of the calculations.

REFERENCES

1. Grasselli, R. K., Burrington, J. D., and Brazdil, J. F., *Faraday Discuss. Chem. Soc.* **72,** 203 (1981); Burrington, J. D., Kortisek, C. T., and Grasselli, R. K., *J. Catal.* **87,** 363 (1984).
2. Callahan, J. L., Grasselli, R. K., Milberger, E. C., and Strecker, H. A., *Ind. Eng. Chem. Prod. Res. Dev.* **9,** 134, 1970.
3. Schuit, G. C. A., *J. Less.-Common Met.* **36,** 329 (1974).
4. Sachtler, W. H., and deBoer, N. H., *in* "Proceedings, 3rd International Congress on Catalysis, Amsterdam, 1964," p. 252. Wiley, New York, 1965.
5. Adams, C. R., and Jennings, T. J., *J. Catal.* **2,** 63 (1962); **3,** 549 (1964).
6. Grzybowska, B., Haber, J., and Janas, J., *J. Catal.* **49,** 150 (1977).
7. Burrington, J. D., and Grasselli, R. K., *J. Catal.* **59,** 79 (1979).
8. Firment, L. E., and Ferretti, A., *Surf. Sci.* **129,** 155 (1983).
9. Grzybowska, B., Haber, J., Marczewski, W., and Ungier, L., *J. Catal.* **42,** 327 (1976).
10. Klissurski, D. G., *in* "Proceedings, Climax 3rd International Conference on the Chemistry and Uses of Molybdenum" (H. F. Berry and P. C. H. Mitchell, Eds.), p. 123. Climax Molybdenum Co., Ann Arbor, Mich., 1979.
11. Anderson, A. B., Kim, Y., Ewing, D. W., Grasselli, R. K., and Tenhover, M., *Surf. Sci.* **134,** 237 (1983).
12. Adams, C. L., *in* "Proceedings, 3rd International Congress on Catalysis, Amsterdam, 1964," p. 240. North-Holland, Amsterdam, 1965.
13. Burrington, J. D., Kartisek, C. T., and Grasselli, R. K., *J. Org. Chem.* **46,** 1877 (1981).
14. Shelton, J. R., and Liang, C. K., *J. Org. Chem.* **38,** 2301 (1973).

15. Davydov, A. A., Mikhaltchenko, V. G., Sokolovskii, V. D., and Boreskov, G. K., *J. Catal.* **55,** 299 (1978).
16a. Brazdil, J. F., Mehicic, M., Glaser, L. C., Hazle, M. A. S., and Grasselli, R. K., *in* "Proceedings of the Division of Petroleum Chemistry of the Meeting of the American Chemical Society, Philadelphia, 1984," p. 699; b. Dadyburjor, D. B., Jewur, S. S., and Ruckenstein, E., *Catal. Rev.* **19,** 293 (1979); Bielanski, A., and Haber, J., *Catal. Rev.* **19,** 1 (1979); Keulks, G. W., and Krenzke, L. D., *in* "Proceedings, 6th International Congress on Catalysis, London, 1976 (G. C. Bonds, P. B. Wells, and F. C. Tompkins, Eds.), p. 806. The Chemical Society, London, 1977; Keulks G. W., *J. Catal.* **19,** 232 (1970); Monneir, J. R., and Keulks, G. W., *J. Catal.* **57,** 331 (1979); Dadyburjor, D. B., and Ruckenstein, E., *J. Phys. Chem.* **82,** 1563 (1978).
17. Burrington, J. D., Kartisek, C. T., and Grasselli, R. K., *J. Catal.* **63,** 235 (1980).
18. Fang, H. L., Meister, D. M., and Swofford, R. L., *J. Phys. Chem.* **88,** 410 (1984).
19. Fang, H. L., Swofford, R. L., McDevitt, M., and Anderson, A. B., *J. Phys. Chem.* **89,** 225 (1985).
20. Brazdil, J. F., Suresh, D. D., and Grasselli, R. K., *J. Catal.* **66,** 347 (1980).
21. Thoni, W., Gai, P., and Hirsch, P. B., *J. Less.-Common Met.* **54,** 263 (1977).
22. Gai, P., *Philos. Mag.* [*Part*] *A* **43,** 841 (1981).
23. Hanafi, Z. M., Khilla, M. A., and Abu-El Saud, A., *Rev. Chim. Mineral* **18,** 133 (1981).
24. Hoppmann, G., and Salje, E., *Opt. Commun.* **30,** 199 (1979).
25. Ivanovskii, A. L., Zhukov, V. P., Slepukhin, V. K., Gubanov, V. A., and Shueikin, G. P., *J. Struct. Chem.* **21,** 30 (1980).
26. Debies, T. P., and Rabalais, J. W., *Chem. Phys.* **20,** 277 (1977).
27. van den Elzen, A. F., and Rieck, G. D., *Acta Crystallogr. Sect. B* **29,** 2433 (1973).
28. Van den Elzen, A. F., and Rieck, G. D., *Act. Cryst. B* **29,** 2436 (1973).
29. Chowdhry, U., Ferretti, A., Firment, L. E., Machiels, C. J., Ohuchi, F., Sleight, A. W., and Staley, R. H., *Appl. Surf. Sci.* **19,** 360 (1984).
30. Anderson, A. B., Kang, D. B., and Kim, Y., *J. Am. Chem. Soc.* **106,** 6597 (1984).
31. Anderson, A. B., and Mehandru, S. P., *Surf. Sci.* **136,** 398 (1984).
32. Anderson, A. B., and Ray, N. K., *J. Phys. Chem.* **86,** 488 (1982).
33. Debnath, N. C., and Anderson, A. B., *J. Vac. Sci. Technol.* **121,** 945 (1982).
34. "CRC Handbook of Chemistry and Physics" (C. D. Hodgman, Ed.), Chemical Rubber, Cleveland, 1962.
35. Driscoll, D. J., and Lunsford, J. H., *J. Phys. Chem.* **87,** 301 (1983).